10-5-2009

Reexamine structures and relative stability of medium-sized silicon clusters: Low-lying endohedral fullerene-like clusters Si_{30}-Si_{38}

Soohaeng Yoo
University of Nebraska–Lincoln

Nan Shao
University of Nebraska–Lincoln

Xiao Cheng Zeng
University of Nebraska-Lincoln, xzeng1@unl.edu

Follow this and additional works at: http://digitalcommons.unl.edu/chemzeng

Part of the Chemistry Commons

Reexamine structures and relative stability of medium-sized silicon clusters: Low-lying endohedral fullerene-like clusters Si_{30}–Si_{38}

Soohaeng Yoo, Nan Shao, and X. C. Zeng

Department of Chemistry and Nebraska Center for Materials and Nanoscience,
University of Nebraska–Lincoln, Lincoln, NE 68588, USA

Corresponding author − X. C. Zeng, email xzeng1@unl.edu

Abstract

We report improved results of lowest-lying silicon clusters Si_{30}–Si_{38}. A large population of low-energy clusters are collected from previous searches by several research groups and the binding energies of these clusters are computed using density-functional theory (DFT) methods. Best candidates (isomers with high binding energies) are identified from the screening calculations. Additional constrained search is then performed for the best candidates using the basin-hopping method combined with DFT geometry optimization. The obtained low-lying clusters are classified according to binding energies computed using either the Perdew–Burke–Ernzerhof (PBE) functional or the Becke exchange and Lee–Yang–Parr correlation (BLYP) functional. We propose to rank low-lying clusters according to the mean PBE/ BLYP binding energies in view that the PBE functional tends to give greater binding energies for more compact clusters whereas the BLYP functional tends to give greater binding energies for less compact clusters or clusters composed of small-sized magic-number clusters. Except for Si_{30}, the new search confirms again that medium-size silicon clusters Si_{31}–Si_{38} constructed with proper fullerene cage motifs are most promising to be the lowest-energy structures.

1. Introduction

Structures of medium-sized silicon clusters have been investigated by many researchers over the last five years [1–20] using various global optimization methods [21–26]. Numerous theoretical studies of medium-sized neutral clusters Si_N in the size range N = 25–40 have shown that beyond N = 29, compact and spherical-like structures are more stable than elongated structures [4, 8, 11, 12, 15] and that carbon fullerene cages tend to be generic *cage motifs* for low-lying spherical-like clusters [4, 9, 11–13, 15–20]. To date, a large population of low-energy clusters of Si_N (N = 25–40) have been obtained from independent global-minimum searches by several research groups: (1) an unbiased search [4] using genetic algorithm [21] combined with the non-orthogonal tight-binding method [27]. (2) an unbiased search [11, 12] using minima-hopping method [25] combined with the density-functional based tight-binding (DFTB) model [28], and (3) various biased searches (based on a large number of pre-constructed endohedral fullerene structures) using a compression method [20] combined with a tight-binding model of silicon [29], or a relaxation method combined with quantum molecular dynamics simulation [16], or a basin-hopping method combined with density-functional theory (DFT) geometry optimization [4, 8, 26]. Although for each size there are many candidates to compete for the lowest-energy structure, the homologue carbon cage motifs (carbon fullerenes [30]) and the number of core atoms inside the cages for most low-ly-

ing clusters are reasonably established [11, 13, 16, 20]. Still, a challenge is to determine exact structures of the lowest-energy clusters (global minima). The challenge is mainly due to two subtleties: (1) high-level *ab initio* computation is very demanding or impractical for medium-sized silicon clusters [31], and (2) the energy rankings based on DFT total-energy computation can be sensitive to the density functional selected, such as the Perdew–Burke–Ernzerhof (PBE) functional [32], or the Becke exchange and Lee–Yang–Parr correlation (BLYP) functional [33]. In general, the PBE functional tends to give greater binding energies for more compact clusters (clusters with smaller cages but more core-filling atoms) whereas the BLYP functional tends to give greater binding energies for less compact clusters or clusters consisting of small-sized magic-number clusters such Si_6, Si_7 and Si_{10} [12, 13].

2. Method and calculation

In this Letter, we present a systematic study of low-lying clusters Si_N (N = 30–38). First, we have collected a large number of low-energy clusters reported in the literature by various groups [4, 11, 13, 16, 20]. Binding energies of these low-energy isomers are computed using DFT methods within generalized-gradient approximation (GGA) implemented in the CPMD program [34]. For the binding-energy computation, we used a supercell length of 25 Å and an energy cut-off of 30 Rydberg for plane-wave expansion. We adopted Troullier–Martins norm-conserving pseudopoten-

Table 1. Optimal core/cage combination for low-lying endohedral silicon clusters Si_{30}–Si_{40} reported in Ref. [16] (Ma et al.) and Ref. [20] (Zhou and Pan). The binding energies per atom are calculated at DFT level with two GGA functionals (PBE and BLYP). Isomers with the greatest PBE binding energy are highlighted in bold, and isomers with the greatest mean (PBE + BLYP) binding energy are highlighted with a frame. The **si36-O′** is obtained from structural perturbation of **si36-O**.

	Optimal core/cage combination (homologue carbon fullerene cage [30])	Binding energy (eV/atom)		
		CPMD/PBE	CPMD/BLYP	Mean
si30-O (Ref. [20])	$Si_4@Si_{26}$ [$C_{26}(D_{3h}{:}1)$]	**3.914**	3.325	3.620
si30-Ma (Ref. [16])	$Si_2@Si_{28}$ [$C_{28}(D_2{:}1)$]	3.886	3.322	3.604
si31-O	$Si_3@Si_{28}$ [$C_{28}(T_d{:}2)$]	**3.918**	3.346	3.632
si31-Ma	$Si_3@Si_{28}$ [$C_{28}(T_d{:}2)$]	3.903	3.338	3.620
si32-O	$Si_4@Si_{28}$ [$C_{28}(T_d{:}2)$]	3.916	3.340	3.628
si32-Ma	$Si_4@Si_{28}$ [$C_{28}(T_d{:}2)$]	3.906	3.334	3.620
si33-O	$Si_5@Si_{28}$ [$C_{28}(T_d{:}2)$]	**3.940**	3.340	3.640
si33-Ma	$Si_3@Si_{30}$ [$C_{30}(C_{2v}{:}3)$]	3.907	3.340	3.623
si34-O	$Si_6@Si_{28}$ [$C_{28}(T_d{:}2)$]	3.932	3.330	3.631
si34-Ma	$Si_4@Si_{30}$ [$C_{30}(C_{2v}{:}3)$]	3.906	3.346	3.626
si35-O	$Si_5@Si_{30}$ [$C_{30}(C_2{:}2)$]	**3.936**	3.344	3.640
si35-Ma	$Si_3@Si_{32}$ [$C_{32}(C_2{:}1)$]	3.914	3.351	3.632
si36-O	$Si_4@Si_{32}$ [$C_{32}(D_3{:}6)$]	3.936	3.356	3.646
si36-O′	$Si_4@Si_{32}$ [$C_{32}(D_3{:}6)$]	**3.937**	3.354	3.646
si36-Ma	$Si_4@Si_{32}$ [$C_{32}(D_{3d}{:}3)$]	3.922	3.347	3.634
si37-O	$Si_5@Si_{32}$ [$C_{32}(D_3{:}6)$]	3.947	3.353	3.650
si37-Ma	$Si_5@Si_{32}$ [$C_{32}(C_2{:}1)$]	3.926	3.341	3.633
si38-O	$Si_6@Si_{32}$ [$C_{32}(D_3{:}6)$]	3.949	3.341	3.645
si38-Ma	$Si_6@Si_{32}$ [$C_{32}(D_3{:}6)$]	3.936	3.338	3.637
si39-O	$Si_7@Si_{32}$ [$C_{32}(D_3{:}6)$]	3.957	3.336	3.646
si39-Ma	$Si_5@Si_{34}$ [$C_{34}(C_s{:}2)$]	3.941	3.362	3.651
si40-O	$Si_6@Si_{34}$ (having 7 member-ring)	3.955	3.353	3.654
si40-Wang (Ref. [9])	$Si_6@Si_{34}$ [$C_{34}(C_{3v}{:}6)$]	3.943	3.359	3.651

tials [35] for PBE and Goedecker–Teter–Hutter (dual space Gaussian) norm-conserving pseudopotentials [36] for BLYP calculations. Top candidates (isomers with large binding energies) are identified from this screening calculation. Next, additional constrained searches are performed by using the basin-hopping (BH) method combined with DFT geometry optimization [19, 26]. The obtained lowest-energy clusters are classified into three groups: one according to the binding energies computed based on the PBE functional, the second according to the binding energies based on the BLYP functional, and the third according to the mean PBE/BLYP binding energies.

3. Results and discussion

Table 1 shows calculated binding energies of low-lying endohedral clusters Si_N (N = 30–40), reported by Ma et al. [16] and Pan and Zhou [20], respectively, as well as their corresponding homologue carbon cages labeled in the Fowler–Manolopoulos fullerene notation (including the point-group symmetry and the Fowler–Manolopoulos label [30]). These endohedral fullerene-like low-lying clusters were pre-constructed based on an empirical rule [4], that is, the Si_{m+3}/Si_m (m = 1,2,…) is an upper/lower limit for the number of core filling atoms to be enclosed in a Si_{26+2m} fullerene cage. Pan and Zhou employed a compression method combined with a tight-binding model of silicon, while Ma et al. relaxed the clusters using a quantum molecular dynamics method. The compression method seems more effective to generate compact low-lying clusters. The most notable results are the predicted homologue carbon fullerene cage C_{28} for Si_{32} and Si_{33} (a larger C_{30} cage was reported in Ref. [13]) and C_{32} cage for Si_{38} (a larger C_{34} cage was reported in Ref. [13]). With these new cage motifs, our additional BH-DFT/PBE search yields new leading candidates for the lowest-energy clusters of Si_{32} and Si_{38}, respectively, namely, **si32-1a** and **si38-1a** (see Table 2). We also confirm structure of the lowest-energy cluster Si_{33}, namely, **si33-1a**. Pan and Zhou reported new low-lying structures of Si_{30}, Si_{31}, Si_{35} and Si_{36} with slightly improved DFT/PBE binding energies (typically 4–8 meV/atom, which are
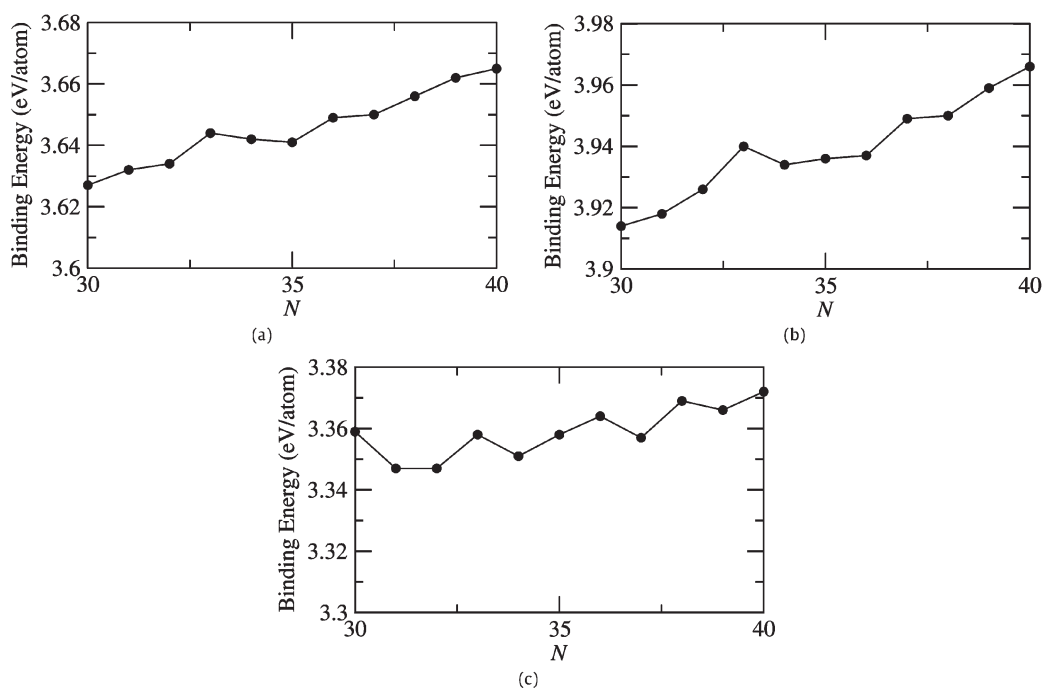
comparable to typical error bar in DFT binding-energy computation ~5 meV/atom). The corresponding homologue carbon fullerene cages (C_{28} for Si_{30} and Si_{31}, C_{30} for Si_{35}, and C_{32} for Si_{36}) are the same in size as reported Refs. 12 and 13. Our additional BH-DFT/PBE search confirms these leading candidates. We thus name them as new **si30-1a**, **si31-1a**, **si35-1a** and **si36-1a**, respectively (see Table 2). We also predict a new leading candidate for the lowest-energy cluster Si_{37}, named as **si37-1a**, whose binding energy is improved by 9 meV/atom (see Table 2 and Reference [13]).

Table 2 also shows new results of low-lying endohedral fullerene-like clusters Si_{31}, Si_{32}, Si_{35}, Si_{36}, Si_{38} and Si_{39} based on DFT/BLYP binding-energy computation, namely, **si31-1a′**, **si32-1a′**, **si35-1a′**, **si36-1a′**, **si38-1a′**, and **si39-1a′**, respectively. In particular, the bind energies of **si32-1a′** and **si36-1a′** are improved by 8 and 10 meV/atom compared to those reported in Ref. [13]. At DFT/BLYP level of theory, the Y-shaped three-arm clusters still give rise to the greatest binding energies for Si_{30}, Si_{32}, Si_{34} and Si_{37}. Except for Si_{30}, however, the binding-energy differences between the Y-shaped three-arm clusters (Ref. [13]) and the endohedral fullerene-like isomers (**si32-1a′**, **si34-1a′** and **si37-1a′**) are less than 6 meV/atom, comparable to the error bar (~5 meV/atom) in DFT energy computation.

In view of the dependence of energy rankings on the functional (e.g., PBE or BLYP) selected, we propose to use the mean (PBE + BLYP) binding energies to rank low-lying silicon clusters. As indicated above, the PBE functional tends to give greater binding energies for more compact clusters whereas the BLYP functional tends to give greater binding energies for less compact clusters or clusters consisting of small-sized magic-number clusters such Si_6, Si_7 and Si_{10}. Hence, to some extent, the mean (PBE + BLYP) binding energy, when used as a measure of relative stability, balances the over preference of compact structure in the PBE calculation and the over preference of less compact structure in the BLYP calculation. The predicted low-lying clusters are also shown in Table 2, where the clusters with the greatest mean (PBE + BLYP) binding energies are highlighted by a frame and plotted in Figure 1(a). For references, the binding-en-

Table 2. Optimal core/cage combination for leading candidates for the lowest-energy clusters Si_{30}–Si_{40} and their binding energies per atom calculated at DFT level with two GGA functionals. "**1a**" denotes the lowest-lying isomer in PBE energy ranking (in bold), "**1a′**" denotes the lowest-lying isomer in BLYP energy ranking (in bold). "**1m**" denotes the isomer with the greatest mean (PBE + BLYP) binding energy. Also, isomers with the greatest mean binding energies are highlighted by a frame.

	Optimal core/cage combination (homologue fullerene cage [30])	Binding energy (eV/atom)		
		CPMD/PBE	CPMD/BLYP	Mean
si30-1a = si30-O	$Si_4@Si_{26}$ [$C_{26}(D_{3h}$:1)]	**3.914**	3.325	3.620
si30-1a′ (Ref. [12])	Y-Shape	3.895	**3.359**	3.627
si31-1a = si31-O	$Si_3@Si_{28}$ [$C_{28}(T_d$:2)]	**3.918**	3.346	3.632
si31-1a′	$Si_3@Si_{28}$ [$C_{28}(T_d$:2)]	3.891	**3.347**	3.619
si32-1a	$Si_4@Si_{28}$ [$C_{28}(T_d$:2)]	**3.926**	3.342	3.634
si32-1a′	$Si_4@Si_{28}$ [$C_{28}(T_d$:2)]	3.919	**3.347**	3.633
si33-1a = si33-O	$Si_5@Si_{28}$ [$C_{28}(T_d$:2)]	**3.940**	3.340	3.640
si33-1a′ (Ref. [13])	$Si_3@Si_{30}$ [$C_{30}(C_{2v}$:3)]	3.931	**3.358**	3.644
si34-1a (Ref. [13])	$Si_4@Si_{30}$ [$C_{30}(C_{2v}$:3)]	**3.934**	3.351	3.642
si35-1a	$Si_5@Si_{30}$ [$C_{30}(C_{2v}$:3)]	**3.936**	3.347	3.641
si35-1a′	$Si_3@Si_{32}$ [$C_{32}(D_3$:6)]	3.907	**3.358**	3.632
si36-1a	$Si_4@Si_{32}$ [$C_{32}(D_3$:6)]	**3.937**	3.355	3.646
si36-1a′	$Si_4@Si_{32}$ [$C_{32}(D_{3d}$:3)]	3.934	**3.364**	3.649
si37-1a	$Si_5@Si_{32}$ [$C_{32}(D_3$:6)]	**3.949**	3.348	3.649
si37-1a′ (Ref. [13])	$Si_5@Si_{32}$ [$C_{32}(D_3$:6)]	3.940	**3.357**	3.649
si37-1m = si37-O	$Si_5@Si_{32}$ [$C_{32}(D_3$:6)]	3.947	3.353	3.650
si38-1a	$Si_6@Si_{32}$ [$C_{32}(D_3$:6)]	**3.950**	3.342	3.646
si38-1a′	$Si_4@Si_{34}$ [$C_{34}(C_{3v}$:6)]	3.940	**3.369**	3.654
si38-1m (Ref. [13])	$Si_4@Si_{34}$ [$C_{34}(C_2$:5)]	3.948	3.364	3.656
si39-1a (Ref. [19])	$Si_5@Si_{34}$ [$C_{34}(C_s$:2)]	**3.959**	3.364	3.662
si39-1a′	$Si_5@Si_{34}$ [$C_{34}(C_s$:2)]	3.945	**3.366**	3.656
si40-1a (Ref. [19])	$Si_6@Si_{34}$ [$C_{34}(C_s$:3)]	**3.966**	3.364	3.665
si40-1a′ (Ref. [19])	$Si_4@Si_{36}$ [$C_{36}(D_{3h}$:13)]	3.928	**3.372**	3.650

Figure 1. Binding energies per atom (eV/atom) of the predicted lowest-energy silicon fullerenes highlighted (in bold or with a frame) in Table 2: (a) mean (PBE + BLYP), (b) PBE, and (3) BLYP binding energies. A distinct peak can be seen at $N = 33$ in (a) and (b).

ergies of the lowest-lying clusters Si_{39} and Si_{40} (see Ref. [19]) are also included in Table 2 and plotted in Figs. 1(a)–(c). Interestingly, only for Si_{30}, the Y-shaped three-arm cluster (**si30-1a′**) still has the greatest mean binding energy. This is likely because the cluster is composed of three highly stable magic-number subunits, i.e. two Si_6 and one Si_{10} (Ref. [12]). For Si_{31}–Si_{40}, the endohedral fullerene-like clusters all give rise to the greatest mean binding energies. Specifically, for Si_{31}, Si_{32}, Si_{35}, Si_{39} and Si_{40}, the corresponding lowest-lying isomers predicted in DFT/PBE calculations also have the greatest mean binding energies, whereas for Si_{33} and Si_{36},

the corresponding lowest-lying isomers predicted in DFT/BLYP calculation have the greatest mean binding energies. As shown in Figs. 1(a)–(c) and Table 2, the leading candidate for Si_{33}, **si33-1a′**, has greater mean binding energy than its two neighbour clusters. Thus, this isomer with $C_{30}(C_{2v}$:3) homologue fullerene cage may be considered in future as a model cluster for the study of chemical reactivity of Si_{33} with small chemical molecules such as C_2H_2 and NO_2 [37].

For Si_{37} and Si_{38}, newly named isomers **si37-1m** [20] and **si38-1m** [13] (see Table 2) neither have the greatest binding energy in

DFT/PBE calculation nor in DFT/BLYP calculation, but both have the greatest mean (PBE + BLYP) binding energy. For Si_{37}, all three leading candidates (**si37-1a**, **si37-1a′** and **si37-1m**) entail the same homologue carbon fullerene cage $C_{32}(D_3{:}6)$, while for Si_{38}, the two leading candidates (**si38-1a′** and **si38-1m**) entail the homologous carbon fullerene cage $C_{34}(C_{3v}{:}6)$ and $C_{34}(C_2{:}5)$, respectively.

4. Conclusion

In conclusion, we have performed constrained basin-hopping search for lowest-lying endohedral silicon clusters Si_{30}–Si_{38}, with initial structures screened from a large population of low-energy clusters obtained from previous searches by several research groups using different searching methods. New leading candidates for the lowest-energy clusters are obtained. These candidate clusters are classified into three groups: one according to the binding energies computed based the PBE functional, the second according to the binding energies based on the BLYP functional, and the third according to the mean PBE/BLYP binding energies. This is because the PBE functional tends to give greater binding energies for more compact clusters whereas the BLYP functional tends to give greater binding energies for less compact clusters or clusters composed of small-sized magic-number clusters. Except for Si_{30}, the new BH-DFT search confirms again that medium-size silicon clusters built with proper fullerene cage motifs are most promising to be the lowest-energy structures.

References

[1] A. Sieck, Th. Frauenheim, and K. A. Jackson, *Phys. Status Solidi B* **240** (2003), p. 537.
[2] S. Yoo and X. C. Zeng, *J. Chem. Phys.* **119** (2003), p. 1442.
[3] S. Yoo, X. C. Zeng, X. Zhu, and J. Bai, *J. Am. Chem. Soc.* **125** (2003), p. 13318.
[4] S. Yoo, J. J. Zhao, J. L. Wang, and X. C. Zeng, *J. Am. Chem. Soc.* **126** (2004), p. 13845.
[5] N. N. Nair, T. Bredow, and K. Jug, *J. Comput. Chem.* **25** (2004), p. 1255.
[6] S. Ma, G. Wang, J. Wang, and L. Xue, *Phys. Lett. A* **337** (2005), p. 216.
[7] J. Zhao, J. Wang, J. Jellinek, S. Yoo, and X. C. Zeng, *Eur. Phys. J. D* **34** (2005), p. 35.
[8] S. Yoo and X. C. Zeng, *J. Chem. Phys.* **123** (2005), p. 164303.
[9] J. Wang, X. Zhou, G. Wang, and J. Zhao, *Phys. Rev. B.* **71** (2005), p. 113412.
[11] J. Bai, L. -F. Cui, J. Wang, S. Yoo, X. Li, J. Jellinek, C. Koehler, T. Frauenheim, L. -S. Wang, and X. C. Zeng, *J. Phys. Chem. A* **110** (2006), p. 908.
[12] S. Yoo and X. C. Zeng, *J. Chem. Phys.* **124** (2006), p. 054304.
[13] S. Yoo, N. Shao, C. Koehler, Th. Frauenheim, and X. C. Zeng, *J. Chem. Phys.* **124** (2006), p. 164311.
[14] R. L. Zhou and B. C. Pan, *Phys. Rev. B* **73** (2006), p. 045417.
[15] O. Ona, V. E. Bazterra, M. C. Caputo, J. C. Facelli, P. Fuentealba, and M. B. Ferraro, *Phys. Rev. A* **73** (2006), p. 053203.
[16] L. Ma, J. Zhao, J. Wang, B. Wang, and G. Wang, *Phys. Rev. A* **73** (2006), p. 063203.
[17] R. L. Zhou and B. C. Pan, *Phys. Lett. A* **368** (2007), p. 396.
[18] J. Wang, J. Zhao, L. Ma, and G. Wang, *Eur. Phys. J. D* **45** (2007), p. 289.
[19] S. Yoo, N. Shao, and X. C. Zeng, *J. Chem. Phys.* **128** (2008), p. 104316. **F**
[20] R. L. Zhou and B. C. Pan, *Eur. Phys. J. D* **47** (2008), p. 367.
[21] K. -M. Ho, A. A. Shvartsburg, B. Pan, Z. -Y. Lu, C. -Z. Wang, J. G. Wacker, J. L. Fye, and M. F. Jarrold, *Nature* **392** (1998), p. 582.
[22] D. J. Wales and H. A. Scheraga, *Science* **285** (1999), p. 1368.
[23] I. Rata, A. A. Shvartsburg, M. Horoi, Th. Frauenheim, K. W. M. Siu, and K. A. Jackson, *Phys. Rev. Lett.* **85** (2000), p. 546.
[24] K. A. Jackson, M. Horoi, I. Chaudhuri, T. Frauenheim, and A. A. Shvartsburg, *Phys. Rev. Lett.* **93** (2004), p. 013401.
[25] S. Goedecker, *J. Chem. Phys.* **120** (2004), p. 9911.
[26] S. Yoo and X. C. Zeng, *Angew. Chem. Int. Ed.* **44** (2005), p. 1491.
[27] M. Menon and K. R. Subbaswamy, *Phys. Rev. B* **50** (1994), p. 11577.
[28] D. Porezag, Th. Frauenheim, Th. Köhler, G. Seifert, and R. Kaschner, *Phys. Rev. B* **51** (1995), p. 12947.
[29] C. Z. Wang, B. C. Pan, and K. M. Ho, *J. Phys. : Condens. Matter* **11** (1999), p. 2043.
[30] P. W. Fowler and E. D. Manolopoulos, An Atlas of Fullerenes, Clarendon, Oxford, UK (1995).
[31] X. Zhu, X. C. Zeng, Y. Lei, and B. Pan, *J. Chem. Phys.* **120** (2004), p. 8985.
[32] J. P. Perdew, K. Burke, and M. Ernzerhof, *Phys. Rev. Lett.* **77** (1996), p. 3865.
[33] A. D. Becke, *Phys. Rev. A* **38** (1988), p. 3098; J. P. Perdew, *Phys. Rev. B* **33** (1986), p. 8822; C. Lee, W. Yang, and R. G. Parr, *Phys. Rev. B* **37** (1988), p. 785;
[34] J. Hutter, A. Alavi, T. Deutsch, M. Bernasconi, S. Goedecker, D. Marx, M. Tuckerman, and M. Parrinello, CPMD, VERSION 3. 7. 1, MPI für Festkörperforschung Stuttgart, 2001.
[35] N. Troullier and J. L. Martins, *Phys. Rev. B* **43** (1991), p. 1993.
[36] S. Goedecker, M. Teter, and J. Hutter, *Phys. Rev. B* **54** (1996), p. 1703; C. Hartwigsen, S. Goedecker, and J. Hutter, *Phys. Rev. B* **58** (1998), p. 3641.
[37] J. L. Elkind, J. M. Alford, F. D. Weiss, R. T. Laaksonen, and R. E. Smalley, *J. Chem. Phys.* **87** (1987), p. 2397; S. Maruyama, L. R. Anderson, and R. E. Smalley, *J. Chem. Phys.* **93** (1990), p. 5349.